TB29

19th International Symposium of Ballistics, 7–11 May 2001, Interlaken, Switzerland

OBSERVATIONS ON THE RATIO OF IMPACT ENERGY TO CRATER VOLUME (E/V) IN SEMI-INFINITE TARGETS

R. Subramanian, S. Satapathy, D. Littlefield

The Institute for Advanced Technology, 3925 W. Braker Ln., Austin, Texas 78759, USA

The ratio of impact energy to crater volume (E/V) is a measure of the work done on the target to create crater volume. This ratio, however, neglects energy dissipated in deformation of the penetrator. In this paper we show, analytically and in hydrocode simulations, that this fraction of energy is non-negligible at lower velocities and acconnts for a portion of the observed velocity dependence.

INTRODUCTION

In the penetration of semi-infinite targets the ratio of impact energy to resultant crater volume (E/V) is a measure of the efficiency of crater formation. While efficiency in this sense does not necessarily imply efficiency in penetration depth (typically quantified as penetration per cube root of impact energy, $P/E^{1/3}$), it nevertheless is a useful metric. Proposed to be an inherent property of the target material [1], experimental data show that it is a function the properties of the penetrator material as well as the impact velocity [2].

However, relating the impact energy to the work done in creating the crater implicitly assumes that the energy spent in deformation of the penetrator is negligible. Alekskeevski [3] noted that some account be made for the energy lost in this deformation process and various authors have shown that this energy can be a non-negligible fraction of the impact energy [4,5]. Nevertheless, energy-based penetration and cavity growth models typically assume a direct transfer of kinetic energy from the penetrator to work done in the target, e.g., [6].

In this paper we examine more closely the energy spent in deformation of the penetrator and its effect on the ratio of impact energy to crater volume (E/V). A brief review of previous work is given and simple analytical estimates are made of the fraction of impact energy spent in penetrator deformation. The results are compared with simulations of monolithic tungsten projectiles impacting semi-infinie steel targets.

BACKGROUND

In the development of theoretical models for the penetration of shaped charge jets it was proposed that the ratio of impact energy to crater volume (E/V) was a material property of the target [1]. Often expressed in the units kilojoules per cubic centimeter (KJ/cc), this quantity is numerically equivalent to stress measured in GPa and hence has been considered as a strength property of the target material.

Experimental data, however, show that E/V is a function of both the impact velocity and penetrator geometry [2]. For monolithic penetrators, lower aspect ratios (e.g., spheres) are more efficient at creating volume than higher aspect ratios (e.g. rods). Both types of penetrators show trends of decreasing E/V (i.e., increasing efficiency) with increasing impact velocity, although it is not clear whether this is an asymptotic approach to a common value or a minimum in the E/V versus velocity curve.

An alternate analysis has been developed that suggests E/V is also related to the ratio of densities. This model, originally developed for hydrodynamic penetration, has been extended to include the effect penetrator strength [6]. In this approach, velocity dependence is derived from a factor "K" that accounts for penetration velocities less than hydrodynamic. The momentum-based Tate/Alekseevski model is used to estimate this factor.

The effect of penetrator strength has been explored by various researchers [7,8]. Although the higher strength penetrators initially have a higher penetration efficiency (dP/dL) this decreases as the projectile decelerates and as penetrator material builds up at the bottom of the crater, referred to as the projectile flow effect.

PENETRATOR DEFORMATION ENERGY

The purpose of this section is to estimate, analytically, the energy spent in deforming the penetrator material and relate this quantity to the available energy. Two methods will be used to estimate this quantity; both will assume a fully eroding projectile and an elastic, perfectly-plastic material model.

A Simple Model

For the large strains experienced by the penetrator material the energy spent in deforming this material is primarily plastic work, the product of the total plastic strain (ε) and the flow stress (Y). Normalizing the deformation energy (E_p) by the impact energy (E_o) yields:

$$\frac{E_p}{E_o} = \frac{2\varepsilon Y}{\rho v^2} \tag{1}$$

where ρ is the density of the penetrator material and v is the impact velocity. While this estimate is arguably crude, it emphasizes the velocity dependence of the fraction of impact energy absorbed by the penetrator.

Cavity Expansion Model

The simple model described above provides a first-order estimate of the velocity dependence of the fraction of impact energy spent in deformation of the penetrator material but requires *a prior* assumption of the total plastic strain. A direct estimate of this fraction can be obtained by computing the energy spent in deforming the penetrator material from the initial solid circular rod form to the final expanded tubular form. Although the actual deformation process is complex, cavity expansion analysis can be used to estimate the energy expended in this process.

Cavity expansion analysis has been used to compute the energy expended in creating crater volume (E/V) [9]. The work done in opening a cavity from zero radius is derived in either cylindrical or spherical coordinates with actual process assumed to lie between these two estimates.

For the present analysis we examine cavity expansion within a finite volume of penetrator material surrounded by an infinite space of target material. The energy expended in deformation of the penetrator is the difference between the work done opening this cavity and the work done on the surronnding target material. The projectile (fully plastic) occupies the radial position from *a* to *b* and the plastically yielded section of the target occupies the radial position from *b* to *c*. The region beyond c is the elastic region in the target. In cylindrical coordinates the radial stress at the elastic-plastic boundary can be shown to be $Y_t/2$ with a Tresca yield criterion. The equilibrium equation in the plastic regions is given by

$$d\sigma_r = -\frac{Ydr}{r}. \tag{2}$$

Integrating this equation from *a* to *b* and from *b* to *c* and using continuity of stresses at the boundaries one obtains

$$\sigma_r\big|_{r=a} = \left[\frac{Y_t}{2} + Y_t \ln\frac{c}{b}\right] + Y_p \ln\frac{b}{a}. \tag{3}$$

The sum in the square brackets is equal to the static cavity expansion pressure in the target material. Hill has shown that this term is equal to the energy expended in creating a cavity of unit volume, inespective of the mode of formation of cavity [9]. Thus the last term in the r.h.s. gives the additional energy required to expand the penetrator material. Thus, the work done in deformation of the projectile is given by,

$$\frac{E_p}{V_p} = \frac{1}{\pi b_0^2}\left[\int_{b_o}^{b_f} \sigma_b 2\pi b db - \int_0^{a_f} \sigma_a 2\pi a da\right]. \tag{4}$$

Assuming incompressibility in both penetrator and the target materials ($b_0^2 = b^2 - a^2$),

$$\frac{E_p}{V_p} = \int_0^{a_f} (\sigma_b - \sigma_a) a da = \frac{2Y_p}{b_0^2}\left[\int_{b_0}^{b_f} b \ln b db - \int_{a_o}^{a_f} a \ln a da\right] = \frac{Y_p}{2}\left[\ln\left(1 + \frac{a_f^2}{b_0^2}\right) + \frac{a_f^2}{b_0^2}\ln\left(1 + \frac{b_0^2}{a_f^2}\right)\right]. \tag{5}$$

The subscripts *o* and *f* correspond to the initial and final radii. A similar derivation can be made in spherical coordinates, which results in:

$$\frac{E_p}{V_p} = \frac{2Y_p}{3}\left[\ln\left(1+\frac{a_f^3}{b_0^3}\right)+\frac{a_f^3}{b_0^3}\ln\left(1+\frac{b_0^3}{a_f^3}\right)\right]. \quad (6)$$

To compute the work expended in cavity expansion using either of these equations the ratio of final cavity radius to the initial rod radius is required. We use a curve fit to data for tungsten into steel [11] given by [12], where the impact velocity, *V*, is given in km/s:

$$\frac{a_f}{b_0} = 1 + 0.287V + 0.148V^2 . \quad (7)$$

The estimates provided by (5, 6) can be normalized by the impact energy, $\rho V^2/2$, to obtain values corresponding to those given by (1). Comparison of these estimates will be made with results from the simulations in the Discussion section.

CTH SIMULATIONS

Simulations were performed using the Eulerian wavecode CTH [13]. Three penetrator geometries (L/D 1, 10, and 30) were evaluated at three impact velocities (1.5, 3.0 and 4.5 km/s). All of the penetrators were right-circular cylinders with a diameter of 1.0 cm. The Johnson-Cook model was used for both the tungsten penetrators and the steel targets with material properties taken from [14].

During the penetration process the impact energy is partitioned between between the penetrator and the target materials and exists either as kinetic, elastic (stored), or plastic energy. The simulations allow tracking the process of this conversion (see, for example, [4,5]) but our interest here is in the final partioning of the impact energy between the two materials. At the end of the penetration event the residual kinetic energy is minimal and the bulk of the energy exists as internal energy. In the target material it is divided between energy dissipated as heat during plastic deformation and elastic energy stored in the surrounding material. In the penetrator material it exists primarily as thermal energy generated during deformation. Table 1 lists the impact energy (E_o) of the penetrator and the final internal energy in the penetrator and target (E_p and E_t). Ideally, the sum of the internal energy in the penetrator and the target materials should equal the impact energy. For the rod type penetrators the sum is ~95% of the impact energy; for the L/D 1 projectiles it is only ~85%. A portion of this discrepancy (~3%) stems from numerical-based errors. The discrepancies are a result of the slight advection errors in energy which get magnified when the reference state for the energy is shifted at the end of the calculation (the energies listed in Table 1 were shifted so that the internal energies for the projectile and target were initially zero). Unfortunately, the equation-of-state library in CTH does not allow independent control of the energy reference state so these errors were unavoidable.

Also measured in the simulations was the resultant crater volume in the target material. As is typically done in experimental measurements, this volume was measured to the original impact plane and hence does not include the volume enclosed by the lip of target material pushed up around the entrance crater. These volumes, normalized by the initial

penetrator volume, are listed in the final column of Table 1. It should be noted that nearly all of the initial penetrator material remained within the crater volume. The normalized crater volumes listed include this material, i.e., the crater volumes were measured as if the residual penetrator material was not present.

Table 1. Energy partitioning and crater volume from CTTI calculation

L/D	Vi (km/s)	Eo (KJ)	Ep (KJ)	Et (KJ)	Vc/Vp
1	1.5	14.9	1.63	18.8	3.98
	3.0	59.5	2.43	49.0	17.3
	4.5	134	3.70	107	37.8
10	1.5	152	20.0	128	3.05
	3.0	610	23.3	561	15.0
	4.5	1372	27.2	1265	36.4
30	1.5	458	71.0	364	2.33
	3.0	1832	69.6	1705	13.1
	4.5	4131	80.0	3851	33.7

DISCUSSION

The ratio of impact energy to crater volume obtained in the simulations is listed in Table 2 as E_o/V_c. These values are plotted in Fig. 1 as a function of impact velocity for the three projectile types. Also included in this plot are experimental data from [11, 15]. The overall trend of the simulations matches the experimental data, namely a decrease in E/V with impact velocity and an L/D effect in which higher aspect ratio projectiles are less efficient at creating crater volume. Our purpose here is to verify that the simulations reasonably match experimental data.

Table 2. Normalized energies from CTH simulation

L/D	Vi (km/s)	Eo/Vc (GPa)	Et/Vc (GPa)	Ep/Vp (GPa)	Ep/Eo
1	1.5	4.76	6.00	2.07	0.11
	3.0	4.38	3.60	3.10	0.04
	4.5	4.51	3.61	4.72	0.03
10	1.5	6.37	5.33	2.55	0.13
	3.0	5.16	4.75	2.97	0.04
	4.5	4.80	4.43	3.46	0.02
30	1.5	8.33	6.62	3.01	0.16
	3.0	5.94	5.53	2.95	0.04
	4.5	5.21	4.85	3.40	0.02

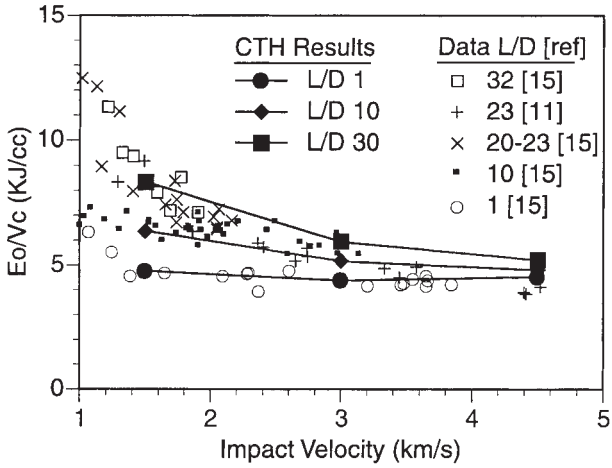

Figure 1. E/V from the CTH simulations and literature data.

The internal energy in the penetrator material is listed in Table 2 as E_p/V_p and plotted as a function of impact velocity in Fig. 2. This quantity increases slightly with increasing impact velocity, but it is essentially constant as noted by other researchers. The exception is the energy spent in deforming the L/D 1 projectile which increases significantly. In all cases, however, the value is greater than the flow stress suggesting a final plastic strain of approximately 1.5. Also included on this figure are the estimates provided by the cylindrical and spherical cavity expansion models (5, 6). An average strength, Y, of 1.8 GPa was used to account for the strain hardening included in the Johnson-Cook material model. The analysis follows the simulations reasonably well, with the cylindrical model more closely matching the computational results.

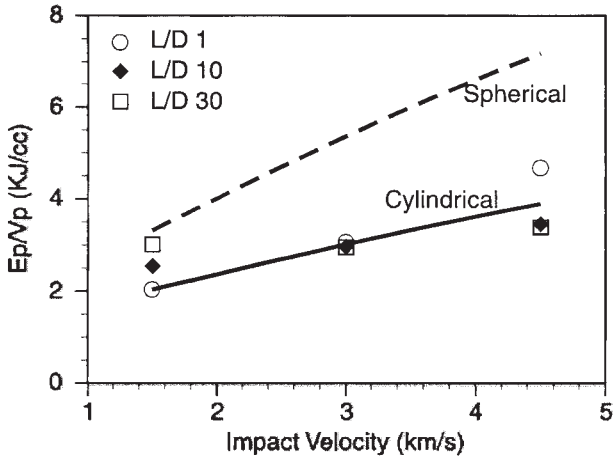

Figure 2. Energy spent in penetrator deformation.

Because energy spent in deforming the penetrator material remains relatively constant it becomes a decreasing fraction of the impact energy. This trend is shown in Fig. 3, in which E_p/E_o obtained in the simulations is plotted as a function of impact velocity. Also included in this figure are the analytical estimates derived above.

Finally, Fig. 4 shows the ratio of internal energy in the target to resultant crater volume (E_t/V_c). It is this quantity that cavity expansion analysis argues is an inherent material property of the target. Nevertheless, there still exists an L/D effect and some velocity dependence is evident.

CONCLUSIONS

The ratio of impact energy to crater volume has been a part of theoretical penetration mechanics for many years. Although originally postulated to be a basic material property of the target, experiments have shown it to be somewhat dependent on the properties and geometry of the projectile. Most significantly it varies with impact velocity, increasing significantly for rod type projectiles at the low velocity.

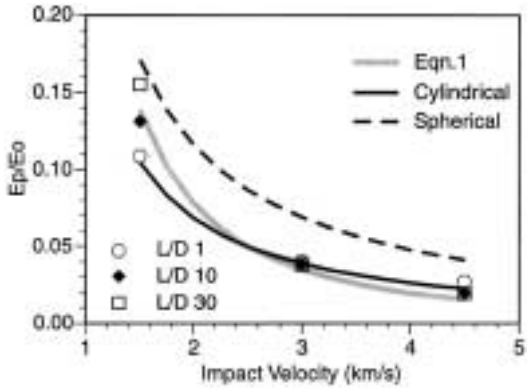

Figure 3. Fration of impact energy spent on penetrator deformation.

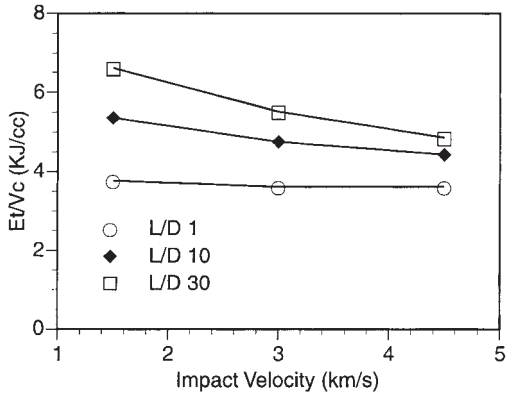

Figure 4. Internal energy in target material normalized by crater volume.

It is perhaps obvious that some portion of impact energy is expended in deforming the penetrator and hence is not available to perform the work required in forming the crater in the target material. Nevertheless, this effect is generally neglected in energy-based penetration modeling. At sufficiently high velocities this assumption is valid, but as these models are applied to lower velocity impacts the effects are no longer negligible. Projectiles with high strength to density ratios will magnify this effect.

Acknowledgements – The authors appreciate the efforts of Paul Bauman for performing the computations. This work was sponsored by the U.S. Army Research Laboratory under contract DAAA21-93-C-O101.

REFERENCES

1. D. R. Christman and J. W. Gehring, "Analysis of High-velocity Projectile Penetration Mechanisms," J. Appl. Phys. 37 (4) (1966)
2. M. J. Murphy, "Survey of the Influence of Velocity and Material Properties on the Projectile Energy/Target Hole Volume Relationship," 10th ISB, San Diego, USA (1987)
3. V. P. Alekseevski, "Penetration of a Rod into a Target at High Velocity," Fizika Goreniya i Vzryva, Vol.2, No. 2, pp. 99–106, (1966)
4. C. E. Anderson, D. L. Littlefield, and J. D. Walker, "Long Rod Penetration, Target Resistance, and Hypervelocity Impact," Intl. J. Impact Eng. 14 (1993)
5. J. D. Walker, "Hypervelocity Penetration Modeling: Momentum vs. Energy and Energy Transfer Mechanisms," to be published in Intl. J. Impact Eng. (Proceedings of HVIS 2000)
6. T. Szendrei, "Analytical Model for High-Velocity Impact Cratering with Material Strengths: Extensions and Validation," 15th ISB, Jerusalem, Israel (1995)
7. Y. Partom, "Projectile-Flow Effect for Long Rod Penetration," 15th ISB, Jerusalem, Israel (1995)
8. Z. Rosenberg and E. Dekel, "Further Examination of Long Rod Penetration: The Role of Penetrator Strength at Hypervelocity Impacts," Intl. J. Impact Eng. 24 (2000)
9. R. Hill, "The Mathematical Theory of Plasticity," Oxford University Press, London, (1966), p. 106
10. R. Hill, "Cavitation and the Influence of Headshape in Attack of Thick Targets by Non-Deforming Projectiles," J. Mech. Phys. Solids 28 (1980)
11. G. Silsby, "Penetration of Semi-infinite Steel Targets by Tungsten Long Rods at 1.3 to 4.5 km/s," 8th ISB, Orlando, USA (1984)
12. J. D. Walker and C. E. Anderson, "A Time-Dependent Model for Long-Rod Penetration," Intl. J. Impact Eng. 16 (1995)
13. J. M. McGlaun, S. L. Thompson, and M. G. Elrick, "CTH: A Three-Dimensional Shock Wave Physics Code," Intl. J. Impact Eng. 10 (1990)
14. D. L. Littlefield, R. M. Garcia and S. J. Bless, "The Effect of Offset on the Performance of Segmented Penetrators," Intl. J. Impact Eng. 23 (1999)
15. V. Hohler and A. Stilp, "Influence of the Length-to-Diameter Ratio in the range from 1 to 32 on the Penetration Performed of Rod Projectiles," 8th ISB, Orlando, USA (1984)